Depletion Performance of Layered Reservoirs Without Crossflow

Michael J. Fetkovich, SPE, **Mark D. Bradley,*** SPE, **Adonna M. Works,** SPE, and **Thomas S. Thrasher,** SPE, Phillips Petroleum Co.

Summary. This paper presents a study of the rate/time and pressure/cumulative-production depletion performance of a two-layered gas reservoir producing without crossflow. The gas reservoir has produced for more than 20 years at an effectively constant wellbore pressure, thus giving continuously declining rate/time and pressure/cumulative-production data for analysis. The field data demonstrate that Arps depletion-decline exponents between 0.5 and 1 can be obtained with a no-crossflow, layered reservoir description. Rate-vs.-time and pressure-vs.-cumulative-production predictions were developed from both 2D numerical and simplified tank models of a two-layered, no-crossflow system. These results demonstrate the effects of changes in reservoir layer volumes, permeability, and skin on the depletion performance.

Introduction

Of all the papers about noncommunicating layered reservoirs, only a few have attempted to deal with the subject of depletion and long-term production forecasting. Tempelaar-Lietz[1] originally discussed the effect of the oil production rate from a volumetric reservoir with more than one layer. Lefkovits *et al.*[2] modified the Tempelaar-Lietz constant-rate, two-layer, single-phase-liquid depletion equations to account for two layers of unequal thickness. Fetkovich[3] applied the constant-wellbore-pressure, single-phase-liquid solution to rate/time production data from a layered reservoir to demonstrate that when two noncommunicating layers, each characterized by a single-phase-liquid exponential decline, $b=0$, were produced commingled, the result was that b increased to 0.2.

Hypothetical solution-gas-drive reservoir studies for noncommunicating layers were conducted by Keller *et al.*[4] to investigate the effects of recovery efficiency and GOR behavior and by Gentry and McCray[5] to study the effects of producing noncommunicating layers on the decline-curve exponent, b. Both studies used single-cell models that did not include transient effects. In addition, both used a conventional PI relationship, $q=J(\Delta p)$, to define a rate equation, instead of an inflow-performance-rate relationship that is a function of the difference in pressure squared—i.e., $q=J(\Delta p^2)$. By their nature, more sophisticated multiphase-flow studies would still have difficulty in assigning realistic k_{ro} and k_{rg} relationships for each layer. Further, the difficulty in obtaining the necessary field data, such as individual well measured oil and gas rates, frequent bottomhole shut-in pressures, and a nonlinear $\bar{p}$-vs.-N_p relationship presents a serious verification problem. A similar problem exists for a single-phase-liquid situation because few oil reservoirs are totally, or even highly, undersaturated and produced to abandonment by simple liquid expansion. Those that are highly undersaturated often develop strong waterdrives because of the large reservoir-pressure decline with small production volumes. Such fields often are placed immediately under waterflood. The single-phase-liquid solutions of Tempelaar-Lietz, however, could find application in very-high-pressured gas reservoirs.

To date, we know of no published field-case history that illustrates depletion-performance characteristics [other than repeat-formation-tester (RFT) layer pressures] to identify no-crossflow, layered-reservoir behavior. Single-phase volumetric gas fields and wells offer the best opportunity for detection of layered-reservoir responses because only single-phase flow exists. Furthermore, production data are measured separately for each well, and annual shut-in pressures are normally taken, sometimes with 48- or 72-hour deliverability tests.

For the gas reservoir described in this paper, the simplified rate/time and cumulative-production/time equations of Ref. 3 and the $\bar{p}/z$-vs.-G_p equation provided support that we were dealing with a noncommunicating layered reservoir. The field has produced for more than 20 years at effectively a low constant wellbore pressure, thus giving continuous, declining rate/time data for analysis. The total field and individual wells examined in our study exhibited a rate/time depletion-decline exponent approaching 1.0 with very little early-time transient data evident. A gas well producing from a single homogeneous layer at a flowing wellbore pressure near zero has a maximum depletion-decline exponent of 0.5.[3,6]

Further confirmation and greater flexibility were then obtained with a conventional single-cell, pseudosteady-state, gas-forecasting program that combines gas material balance and a stabilized back-pressure curve for each layer. In addition, a fully implicit radial numerical model consisting of two fifty-cell layers was used to simulate annual 72-hour shut-ins and 48-hour deliverability tests and to verify the results obtained from simplified approaches. Throughout this paper, these approaches will be referred to as the backpressure-curve/material-balance and the radial-model methods, respectively. All basic results and conclusions drawn in this paper, however, can be made with any of the approaches described above. In all figures, the simulated 72-hour shut-in points are strictly the product of the radial model; all other results were consistently obtained by both the backpressure-curve/material-balance and the radial-model approaches. Both constant-wellbore-pressure and constant-rate depletion were investigated. Graphical presentations of rate vs. time and pressure vs. cumulative production clearly demonstrate the effects of changes in the reservoir layer volumes, permeability, k, and skin, s, on the depletion performance of a two-layered system without crossflow.

Field Description

Development drilling began in our field of study in 1961; 212 gas wells had been drilled by early 1966. The reservoir consists of about 350 ft of gross sandstone thickness at 1,800 ft. Initial reservoir pressure was about 428 psia. Other parameters include a reservoir temperature of 80°F, an average porosity of 15%, a water saturation of 51%, and a gas gravity of 0.7. A shale barrier averaging 50 ft thick was clearly identified and correlated across the entire field. Core data indicate a bimodal distribution with a permeability ratio between 10:1 and 20:1.

Wells were generally stimulated upon completion with 500 to 1,000 gal of 15% HCl, followed by a sand fracture, which included 20,000 gal of gel and 40,000 lbm of 20/40 sand. **Table 1** shows stimulation results in terms of skin effect along with other results obtained from initial isochronal tests. In most cases, the exponent of the backpressure curve, n, was 1.0. Of the four tests that did not yield a backpressure exponent of 1.0, one is actually a flow-afterflow test, and the others had not adequately cleaned up after stimulation. All our studies are based on the assumption that non-Darcy flow is not present in the reservoir—i.e., $n=1.0$ for each layer.

The field came on production virtually wide open against an essentially constant wellbore pressure. A type-curve analysis and regression fit of the total field rate/time production data yielded $b=0.89$, practically identical to what we later found from individual well analysis. This b value approaching unity first suggested that we were looking at a no-crossflow, layered reservoir, particularly

*Now at Conoco Inc.

TABLE 1—INITIAL ISOCHRONAL TEST RESULTS

Well	Test Date	Test Wellhead Shut-in Pressure, p_{cs} (psig)	3-Hour Isochronal Tests: CAOF* Mcf/D	3-Hour Isochronal Tests: Exponent n	kh (md-ft)	h (ft)	k (md)	s	k_1 (md)	k_2 (md)
A	Oct. 19, 1960	366.6	16,000	1.00	1,498	64	23.4	−4.6	59	5.9
B	Feb. 20, 1961	326.0	14,600	1.00	1,761	29	60.7	−5.2	152	15.2
C	Jan. 27, 1961	351.6	13,700	1.00	1,332	37	36	−4.8	90	9.0
D	Feb. 27, 1961	385.7	6,200	0.78	1,248	47	26.6	−4.0	66	6.6
E	March 6, 1961	379.9	3,600	1.00	332	74	4.5	−3.8	11	1.1
F	March 13, 1961	407.4	8,800	0.83	984	72	13.7	−4.5	34	3.4
G	Jan. 23, 1963	371.7	3,690	0.69**	565	29	19.5	−4.0	49	4.9
H	Aug. 12, 1963	408.7	5,800	1.00	225	39	5.8	−4.8	14	1.4
I	Oct. 2, 1963	417.9	2,000	0.86	215	23	9.3	−4.0	23	2.3
J	Sept. 9, 1963	405.7	5,900	1.00	397	41	9.7	−4.4	24	2.4
Arithmetic averages		382.1	8,029	0.92	856	46	20.9 18.8†	−4.4	52	5.2

$h_1/h_2=1:2$, $k_1/k_2=10:1$; $k_1h_1+k_2h_2=kh_t$; $h_1+h_2=h_t$, $k_1=10k_2$, and $h_2=2h_1$.
*Calculated absolute open flow.
**Flow-afterflow test.
†$\Sigma kh/\Sigma h$.

because both the field and the individual wells had the same decline exponent.

Well Performance

We present rate/time and pressure/cumulative-production data for two typical wells in the field that cover a range of gas in place. **Fig. 1** presents additional field data in the form of a composite log-rate-vs.-log-time overlay of 10 wells. This technique has also been applied to five California Monterey producing fields.[7]

Fig. 2 is a conventional semilog plot of rate/time data for these two wells. The high initial percentage decline rate, decreasing to a much lower present percentage, is characteristic of wells experiencing hyperbolic decline with high decline exponents. As shown in **Fig. 3**, the log-rate-vs.-log-time plots of these wells indicate little, if any, early transient production; the high b values are the result of differential depletion of a layered reservoir.

The shape of the pressure/cumulative-production data (**Fig. 4**) is typical of most other wells in the field. The rather large displacement between the measured annual 72-hour $\bar{p}/z$ points and the straight line connecting the initial and final points was first misinterpreted as the behavior of a low-permeability reservoir. As Table 1 shows, our analysis of available isochronal test data yielded permeability values much too high to explain this departure. These $\bar{p}/z$ shapes are characteristic of a no-crossflow, layered reservoir with a large contrast in layer permeabilities and volumes.

Basic Equations

Rate/Time Equations. With the assumption of Darcy flow, the depletion rate/time decline equation for a gas well[3] producing from any one layer at a constant wellbore pressure of zero, $p_{wf}=0$, is

$$q_g(t)=(q_{gi})_{\max}/\{[(q_{gi})_{\max}/G_i]t+1\}^2. \quad \ldots\ldots\ldots\ldots\ldots (1)$$

Note that the exponent 2 is the reciprocal of the Arps[8] exponent $1/b$; i.e., $b=0.50$. Expressed in terms of reservoir variables, $(q_{gi})_{\max}$ may be defined as

$$(q_{gi})_{\max}=kh(p_i^2)/\{1{,}424(\overline{\mu z})T[\ln(0.472r_e/r_w)+s]\}. \quad \ldots\ldots (2)$$

If a commingled well produces at a constant wellbore pressure, then the flow rate from each layer is independent of the flow rates of all the other layers and the total well production is the sum of all the layers' production. Rate/time decline analysis for a two-layered system is performed with a log-log plot of total flow rate q_{gt} vs. time, where

$$q_{gt}(t)=\frac{(q_{gi})_{\max 1}}{\{[(q_{gi})_{\max 1}/G_{i1}]t+1\}^2}+\frac{(q_{gi})_{\max 2}}{\{[(q_{gi})_{\max 2}/G_{i2}]t+1\}^2}. \quad \ldots\ldots\ldots\ldots\ldots\ldots (3)$$

Only if $(q_{gi})_{\max 1}/G_{i1}=(q_{gi})_{\max 2}/G_{i2}$ will the value $b=0.5$ for each layer yield a composite rate/time value of $b=0.5$.

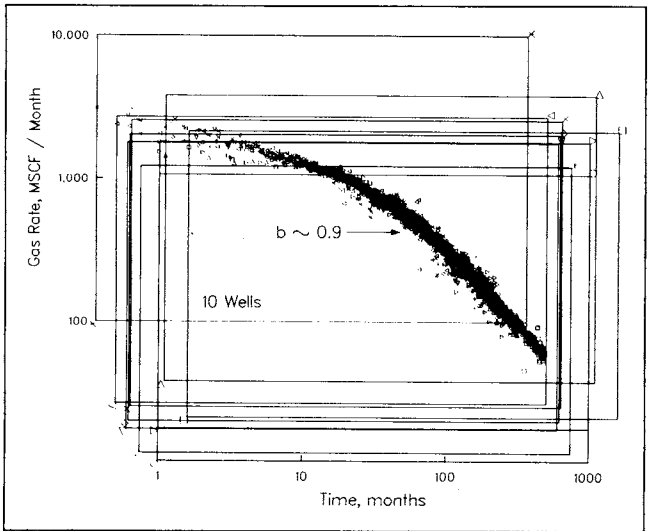

Fig. 1—Overlay of log-rate-vs.-log-time production data of 10 gas wells.

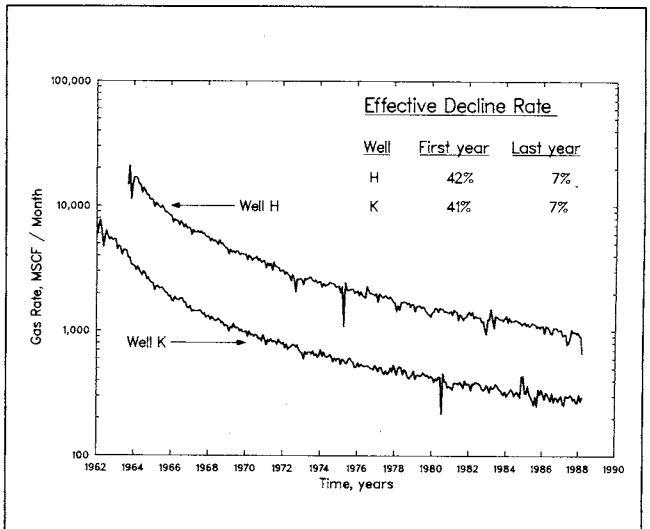

Fig. 2—Semilog plot of rate/time production data.

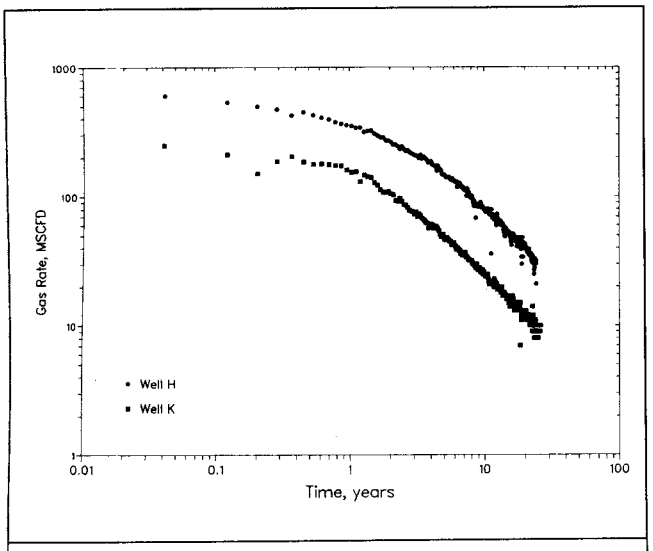

Fig. 3—Log-rate-vs.-log-time production data.

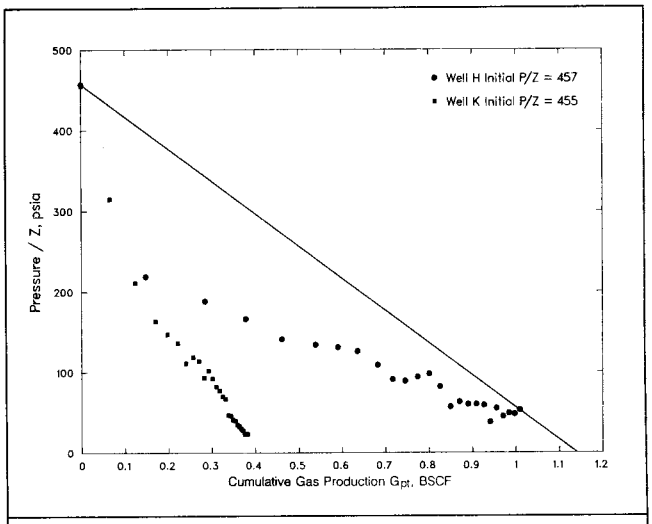

Fig. 4—p/z vs. cumulative production, measured 72-hour shut-ins.

For the limiting case where $(q_{gi})_{max2} \rightarrow 0$ in the low-permeability layer, the total rate/time profile will, of course, be identical to that of the high-permeability layer; each will have a b value of 0.5.

As defined in Ref. 3, the ratio of decline-curve dimensionless time to real time, t_{dD}/t, is equal to $(q_{gi})_{max}/G_i$. Layers having similar values of t_{dD}/t or $(q_{gi})_{max}/G_i$ will deplete at the same rate and could be treated as a single equivalent layer. We will use the ratio

$$[(q_{gi})_{max}/G_i]_R=[(q_{gi})_{max1}/G_{i1}]/[(q_{gi})_{max2}/G_{i2}] \quad \ldots\ldots\ldots (4)$$

as a correlating parameter in our study, along with the layer volume ratio, F_V, defined as G_{i1}/G_{i2}. By convention, Layer 1 is always the more permeable layer.

Assuming that $p_{i1}=p_{i2}$ and $(\mu c_t)_{i1}=(\mu c_t)_{i2}$, and substituting reservoir variables as shown in Ref. 3, we obtain

$$\left[\frac{(q_{gi})_{max}}{G_i}\right]_R=\frac{k_1/\phi_1[\ln(0.472r_{e2}/r_w)+s_2]}{k_2/\phi_2[\ln(0.472r_{e1}/r_w)+s_1]}\frac{{r_{e2}}^2}{{r_{e1}}^2}. \quad \ldots\ldots\ldots (5)$$

Similar ratios were also suggested by Raghavan[9] except for the inclusion of the skin and r_e terms. Note that the assumption of equal initial pressures is not necessary for the constant-wellbore-pressure cases because the layer production rates are independent of each other.

Cumulative-Production/Time Equations. With the assumption of Darcy flow, the cumulative-production/time equation[3] for a gas well producing from any one layer against a constant wellbore pressure of zero is

$$\frac{G_p(t)}{G_i}=1-\frac{1}{\{[(q_{gi})_{max}/G_i]t+1\}}. \quad \ldots\ldots\ldots\ldots\ldots (6)$$

Material-Balance Equation. The material-balance equation for any one layer is

$$(\bar{p}/z)=(p_i/z_i)\{1-[G_p(t)/G_i]\}. \quad \ldots\ldots\ldots\ldots\ldots\ldots (7)$$

For a two-layer system with equal initial pressure and fluids, the equation becomes

$$(\bar{p}/z)_t=(p_i/z_i)\{1-[G_{p1}(t)+G_{p2}(t)]/(G_{i1}+G_{i2})\}. \quad \ldots\ldots\ldots (8)$$

Layered-Reservoir Performance Forecasts

To understand the depletion performance of our noncommunicating layered reservoir better, a one-well, two-layered system was designed from reservoir properties of the gas reservoir described previously. The following data were used for both layers: $r_e=2{,}979$ ft, $r_w=0.30$ ft, $\phi=0.15$, $S_w=0.514$, $\gamma_g=0.7$, $T=80°$F, and $p_i=428$ psia. A total well thickness, h, of 24 ft was used to obtain an average well original gas in place of 1.50 Bscf. All forecasts were made with a minimum bottomhole flowing pressure, p_{wf}, of 42.8 psia, 10% of the initial shut-in pressure. Permeability ratios, F_k, ranging from 1:1 to 1,000:1 were investigated along with layer volume ratios, F_V, of 1:1, 1:2, and 2:1. The low-permeability layer was generally assigned a permeability of 1 md. Various combinations

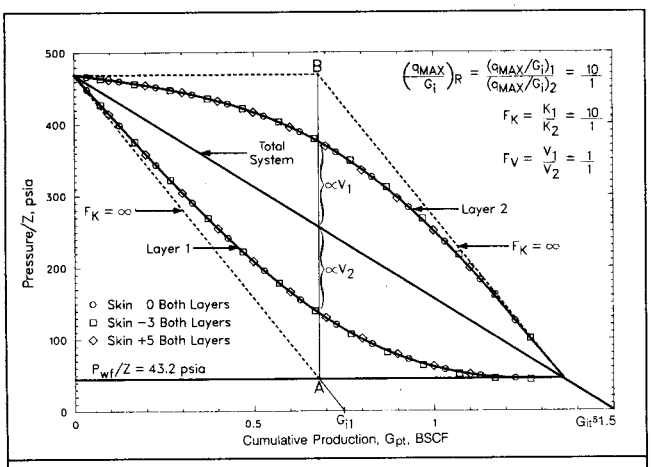

Fig. 5—p/z vs. cumulative production, layer skins equal and $F_V=1$.

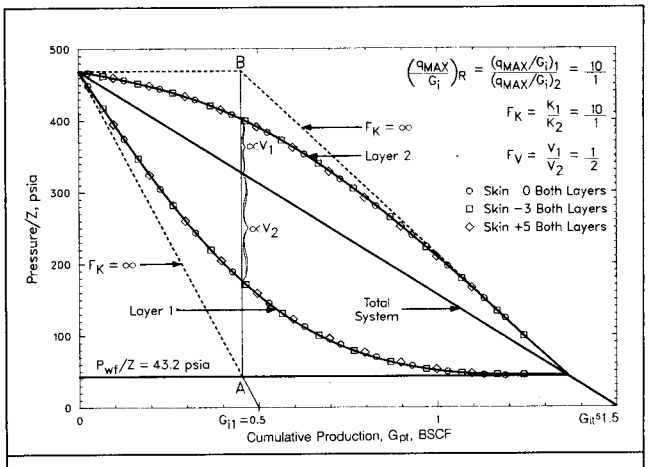

Fig. 6—p/z vs. cumulative production, layer skins equal and $F_V=1:2$.

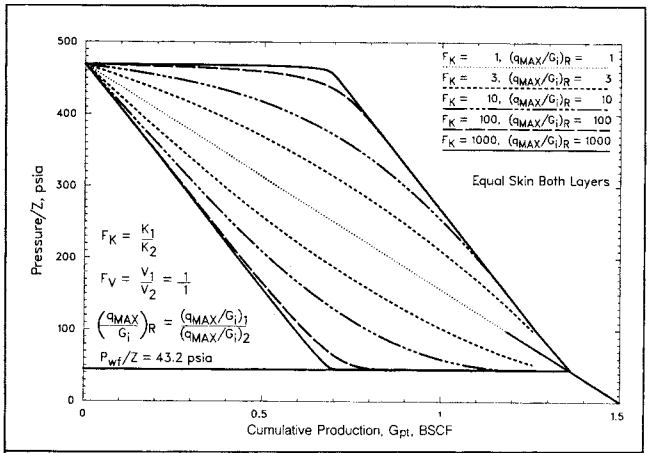

Fig. 7—p/z vs. cumulative production, layer skins equal, $F_V = 1$ and F_k range 1 to 1,000.

of skin, s, of +5, 0, and −3 were also investigated. Realistic constant-rate forecasts were made assuming typical contract rates of take of 1 MMscf/D/8.6 Bscf and 1 MMscf/D/5 Bscf of original gas in place.

Discussion of Results

Pressure/Cumulative-Production Graphs. The pressure/cumulative-production graphs for layered reservoirs are unique because individual layer and total system $\bar{p}/z$ are plotted vs. the total commingled cumulative production from all layers, G_{pt}. This graph can be prepared for any number of layers. **Fig. 5** is such a plot for our two-layered system, assuming $F_V = 1:1$ or 0.750 Bscf/0.750 Bscf. In this case, F_k and $(g_{max}/G_i)_R$ both equal 10 because the skins on both layers are equal (see Eq. 5). Production rates at constant wellbore pressure and two different realistic constant-rate rates of take (1 MMscf/D/8.6 Bscf and 1 MMscf/D/5 Bscf) produced identical results. Note that, for any given F_k, as long as the skins are equal in both layers, differential depletion will be identical for both layers. We also found this to be true for other F_V values. Further, the backpressure-curve/material-balance and radial-model results exactly overlie each other.

Another important observation to be made from Fig. 5 is that with $F_V = 1$, the respective distances between the total system $\bar{p}/z$ and each layer $\bar{p}/z$ are always equal for any value of cumulative production, G_{pt}. Both layer $\bar{p}/z$ values converge at the intersection of the minimum flowing pressure and total system $\bar{p}/z$ lines.

Fig. 5 also demonstrates two limiting conditions: when $F_k = 1$ or $(q_{max}/G_i)_R = 1$, both layers will deplete equally and the $\bar{p}/z$ for each layer will overlie the total system $\bar{p}/z$ curve. At the other extreme, when $F_k \to \infty$, or $(q_{max}/G_i)_R \to \infty$, the maximum differential-depletion envelope is described. The vastly more permeable Layer 1 will totally deplete, while Layer 2 remains at initial pressure; Layer 2 will then deplete after Layer 1 is no longer producing. The envelope can be constructed by first connecting p_i/z_i to G_{i1}. We call the intersection of this line and the horizontal line representing p_{wf}/z Point A. We call the intersection of the vertical line passing through Point A and the horizontal line representing p_i/z_i Point B. Finally, we connect Point B to the point where p_{wf}/z and the total system $\bar{p}/z$ intersect.

TABLE 2—CORRELATION PARAMETER VALUES FOR VARIOUS SKIN COMBINATIONS WHEN $F_k = 10$ and $F_V = 1$

Skin		
Layer 1	Layer 2	$(q_{imax}/G_i)_R$
−3	0	15.5
0	5	15.9
−3	−3	10
0	−3	6.4
5	0	6.3

Observations concerning Fig. 5 also apply to **Fig. 6**. The only difference is that $F_V = 1:2$ in Fig. 6; i.e., Layer 1 contains 0.5 Bscf, while Layer 2 contains 1.00 Bscf. Note that for this F_V, the vertical distance between the total system $\bar{p}/z$ and the Layer 1 $\bar{p}/z$ curve is twice that between the total system $\bar{p}/z$ and the Layer 2 $\bar{p}/z$ curve. By contrast, for $F_V = 2:1$, the distance between the total system and Layer 1 $\bar{p}/z$ curves is half that between the total system and Layer 2 $\bar{p}/z$ curves. In all cases, the vertical distance between the total system $\bar{p}/z$ line and each layer $\bar{p}/z$ curve is inversely proportional to their volume ratios.

A range of F_k from 1 to 1,000 is shown in the pressure/cumulative-production plot of **Fig. 7.** In each case, both layers are assumed to have equal skins and equal volumes. Similar results are obtained for $F_V = 1:2$ and 2:1. The degree of differential depletion between the two layers increases as $(q_{max}/G_i)_R$ increases and decreases as $(q_{max}/G_i)_R$ decreases. As $(q_{max}/G_i)_R$ approaches unity, the system will behave as a single layer.

Unequal Layer Skins. We have assigned a range of skin values to our individual well studies of +5, 0, and −3 to demonstrate the significance of $(q_{max}/G_i)_R$ as a correlation parameter. **Table 2** gives $(q_{max}/G_i)_R$ values obtained for various skin combinations with $F_k = 10$ and $F_V = 1$.

Fig. 8 shows that, when different layer skins result in the same value of $(q_{imax}/G_i)_R$, $\bar{p}/z$-vs.-G_{pt} curves for each layer exactly overlie each other. Similar results are obtained with regard to the decline exponent, b.

Constant-Rate Cases. To investigate the effect of rate sensitivity on differential depletion, three different constant-rate forecasts were

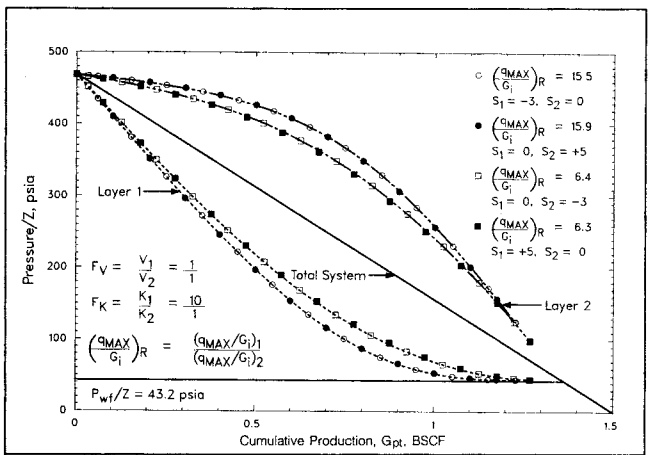

Fig. 8—Effect of different layer skin, s, on p/z-vs.-G_p curves, $F_V = 1$, $F_k = 10$.

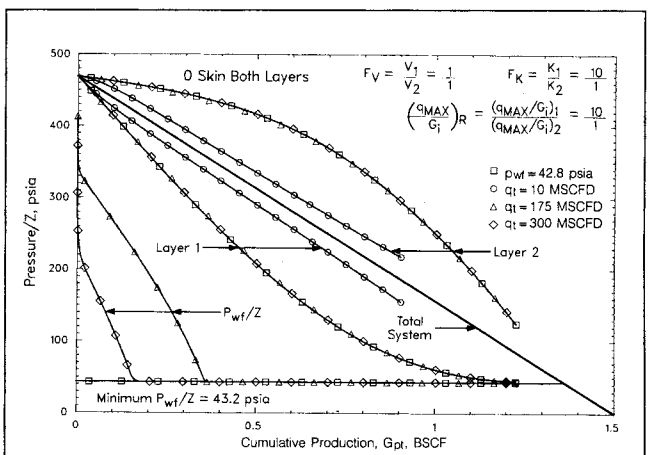

Fig. 9—Effect of rate on differential depletion.

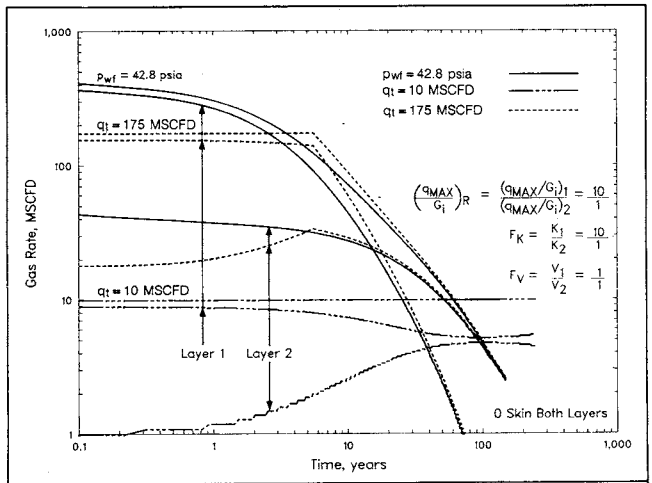

Fig. 10—Layer and composite rates vs. time at constant wellbore pressure and constant rate.

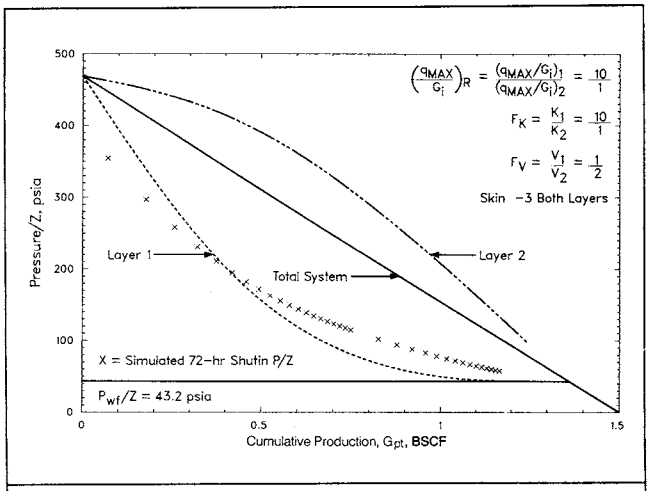

Fig. 11—Simulated 72-hour shut-in *p/z* compared with layer average pressure *p/z*, constant-wellbore-pressure case.

made along with a constant-wellbore-pressure case assuming $F_k=10$, $F_V=1$, and equal layer skins. Initial rates of 300 Mscf/D from a 1 MMscf/D/5 Bscf rate of take, 175 Mscf/D from a 1 MMscf/D/8.6 Bscf rate of take, and 10 Mscf/D, representing an economic limit rate, were forecast.

The $\bar{p}/z$-vs.-G_{pt} plot (**Fig. 9**) demonstrates that differential depletion is not rate-sensitive for our practical rates of interest. This is a result of the gas flow rates being a function of *kh* and a difference in pressures squared; i.e., $q_g=f(\Delta p^2)$. As p_{wf} approaches initial reservoir shut-in pressure ($\Delta p\rightarrow 0$), as is the case for the 10-Mscf/D forecast, the gas rate becomes a function of a difference in pressures, i.e., $q_g=f(\Delta p)$. Tempelaar-Lietz[1] found that for the single-phase-liquid case, where $q_0=f(\Delta p)$, differential depletion was sensitive to all flow rates and that as the constant-rate $q\rightarrow 0$, both layers deplete equally; i.e., Layer 1, Layer 2, and the total system pressures are all equal. Obviously, very-high-pressure gas wells will behave like the single-phase-liquid case, $q=f(\Delta p)$, and solution-gas-drive reservoirs below the bubblepoint should behave like the low-pressure-gas cases because oilwell inflow performance[10] yields $q_0=f(\Delta p^2)$.

Fig. 10 presents individual-layer and composite flow rates for the above cases. Initially, layer rates are a function of *kh*. When the constant-rate cases go on decline, the rates again become a function of *kh*. Note that only for the 10-Mscf/D case do the layer rates approach being equal—the constant-rate definition of pseudosteady state for two layers of equal PV. At practical production rates that eventually decline to the economic rate of 10 Mscf/D, pseudosteady state is never achieved. Even for the 10-Mscf/D case, results obtained from both the backpressure-curve/material-balance and radial-model methods were identical.

Field Shut-in Pressures. Routine field data available from layered gas wells consist of monthly commingled production rates, q_t, total system cumulative production, G_{pt}, and commingled shut-in pressures. In our field of study, 72-hour shut-in pressures are taken annually. On the basis of approximate field reservoir parameters ($F_k=10:1$, $F_V=1:2$, and $s_1=s_2=-3$), the radial model was used to simulate annual 72-hour shut-in and 48-hour drawdown-pressure tests. The constant-wellbore-pressure-case results are shown in **Fig. 11.** As expected, the commingled shut-in pressures divided by z basically follow the $\bar{p}/z$ curve of the more permeable layer. Results obtained for a 175-Mscf/D constant-rate case were similar. The 72-hour pressures for the constant-wellbore-pressure case are initially somewhat lower, however, than those for the constant-rate case because the 72-hour shut-in begins from a much lower flowing pressure before shut-in. After about 0.4 Bscf of recovery, the 72-hour pressure begins to exceed the more permeable layer pressure because of interlayer wellbore backflow.

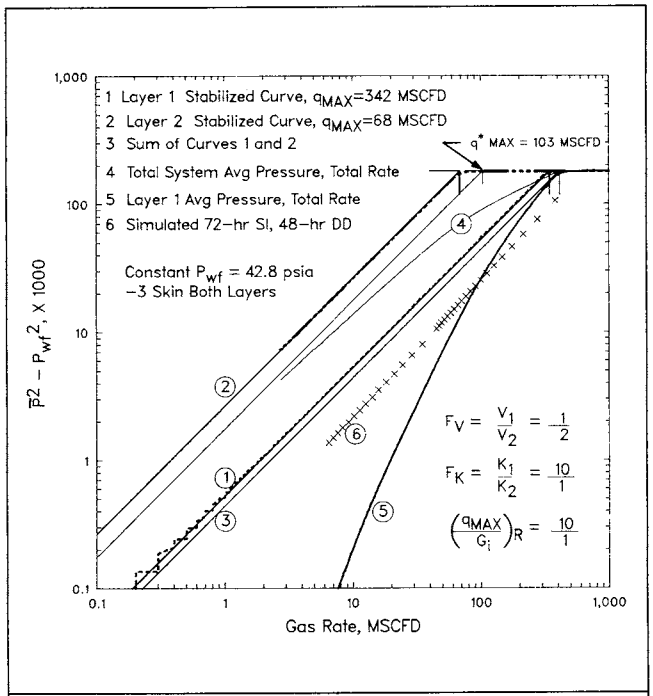

Fig. 12—Layer and composite well backpressure-curve performance, constant wellbore pressure.

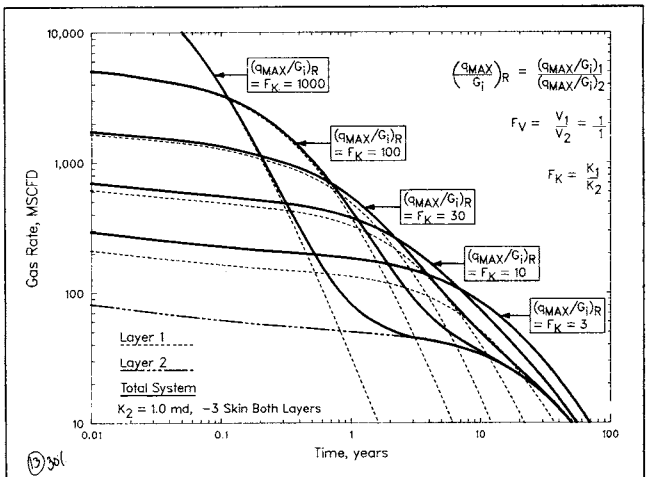

Fig. 13—Effect of changes in $(q_{max}/G_i)_R$ ratio on total system decline for $F_V=1$.

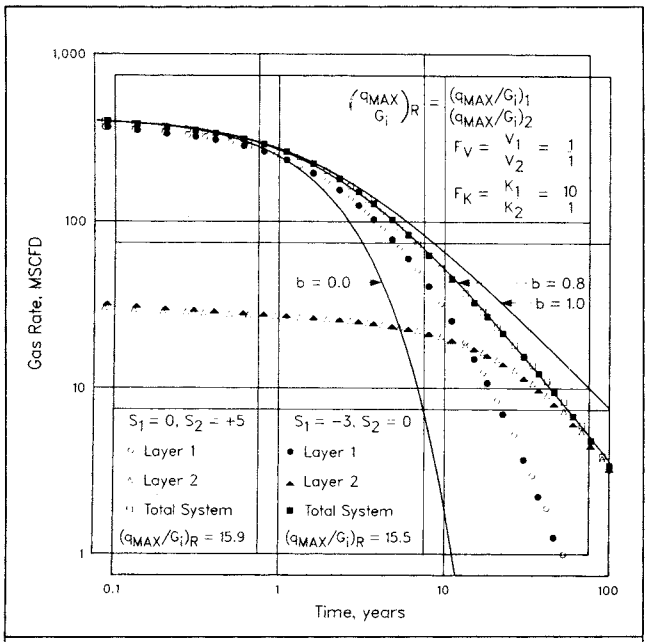

Fig. 14—Effect of layer skins on total system decline exponent *b*, for $F_V = 1$ and $F_k = 10$.

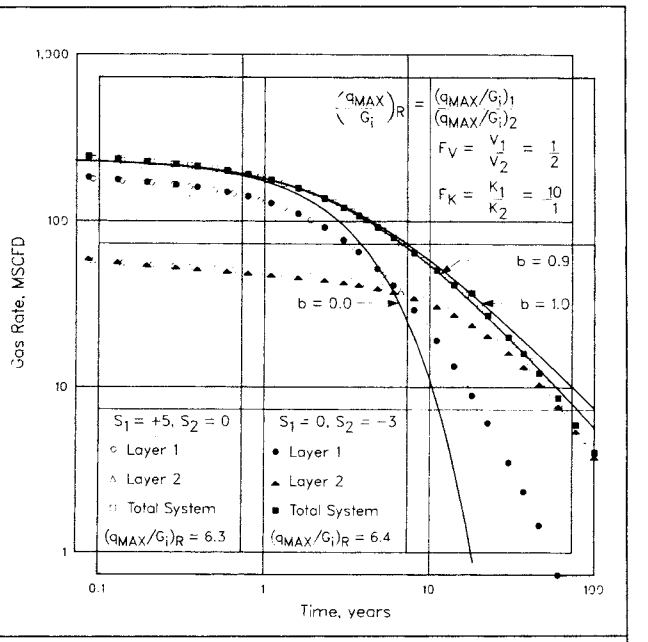

Fig. 15—Effect of layer skins on total system decline exponent *b*, for $F_V = 1:2$ and $F_k = 10$.

TABLE 3—DECLINE EXPONENT *b* AS A FUNCTION OF $[(q)_{max}/G_i]_R$ and F_V

	F_V		
$[(q)_{max}/G_i]_R$	2:1	1:1	1:2
1	0.4	0.4	0.4
3	0.5	0.55	0.6
5	0.6	0.65	0.7
10	0.65	0.8	1.0
15.5	0.65	0.8	1.0
30*	0.6	0.7	0.8
100*	0.5	0.5	0.5
1,000*	0.4	0.4	0.4

*Double depletion decline *b* is for the first depletion decline.

Backpressure Curves

A stabilized backpressure curve and a material-balance equation are frequently used to prepare long-term production forecasts for single-layer systems. The stabilized backpressure curve is used only during constant-wellbore-pressure production—i.e., the declining production period. A single stabilized backpressure-curve relationship for multilayer systems has never been defined, mainly because previous investigations of multilayered systems are based on constant-rate production—i.e., the rate never experiences decline.

Fig. 12 shows several different backpressure curves developed from a radial-model forecast that assumes $F_V = 1:2$, $F_k = 10:1$, $s_1 = s_2 = -3$, and a constant $p_{wf} = 42.8$ psia. Annual 72-hour shut-ins, each followed by a 48-hour drawdown, were also simulated with the radial model to represent typical official test requirements, test data that would normally be available to construct a 48-hour-depletion backpressure curve. The average reservoir pressure, $\bar{p}$, used to define the backpressure curves in Fig. 12 represents either the simulated 72-hour shut-in pressure or the volumetric average pressure for each layer and the total system.

Curve 1 in Fig. 12 represents the calculated position of the stabilized or pseudosteady-state curve for Layer 1 from the reservoir variables previously defined. The points that overlie the curve were obtained from the radial model. The pressure, $\bar{p}$, and rate, q, are those of Layer 1 only.

Curve 2 represents the stabilized backpressure curve for Layer 2, the low-permeability layer. Curve 3 is simply the sum of Curves 1 and 2. Curve 4 represents the stabilized backpressure curve for the total system, where $\bar{p}$ is the volumetric average pressure of the total system and q is the total flow rate for both layers. Clearly, Curve 4 is not a straight line except at low flow rates. We have therefore avoided the expression "pseudosteady state" when describing it. Curve 4 originates at the q_{maxt} of Curve 3 and asymptotically approaches a straight line of unit slope established from the Layer 2 stabilized potential, q_{max2}, and the ratio of layer PV's, such that

$$(q)^*_{max} = (q)_{max2}[(G_{i1} + G_{i2})/G_{i2}]. \quad \ldots\ldots\ldots\ldots\ldots\ldots (9)$$

Because layer flow rates at these low levels become a function only of layer PV's, the position of this straight-line asymptote was independent of layer skins. We were unable to predict the layered-reservoir stabilized-curve limiting position from the constant-rate late-time solution of Ref. 2.

The shape of the total system stabilized curve gives the appearance of a continuous loss in well performance that could be misinterpreted as a changing skin, a loss of reservoir permeability, or an infinite-acting transient decay.

Curve 5 is based on the combined rate from both layers and the volumetric average pressure of the more permeable layer. We expected the commingled shut-in pressure to approach the pressure of the more permeable layer, as in Fig. 11. Curve 6 is a plot of the simulated annual 72-hour shut-in pressure and 48-hour drawdown flow rate obtained while producing against a constant p_{wf} of 42.8 psia. Surprisingly, a straight line with a backpressure-curve exponent of $n = 0.934$ results. (Recall that, for Darcy flow, $n = 1$ is assumed for each layer.) Note that Curve 6, the 48-hour depletion backpressure curve, does not reflect the shape of Curve 4, the layered, stabilized backpressure curve.

Rate/Time Depletion Behavior

Fig. 13 is a comparison of individual layer and total system rate/time responses for various ratios of $(q_{max}/G_i)_R$. Only the contribution of Layer 1, the high-permeability layer, changes from case to case; the permeability of Layer 2 is fixed at 1.0 md in each case. Further, each layer contains a gas in place of 0.75 Bscf, and each has been assigned a skin of -3.

The log-rate-vs.-log-time profile for any single layer can be matched to a depletion *b* stem of 0.4. This result is commensurate with the expected behavior of a dry gas reservoir in the presence of a constant backpressure equal to 10% of the initial reservoir pressure. We have confirmed, however, that a $b = 0.5$ results when $p_{wf} = 0$.

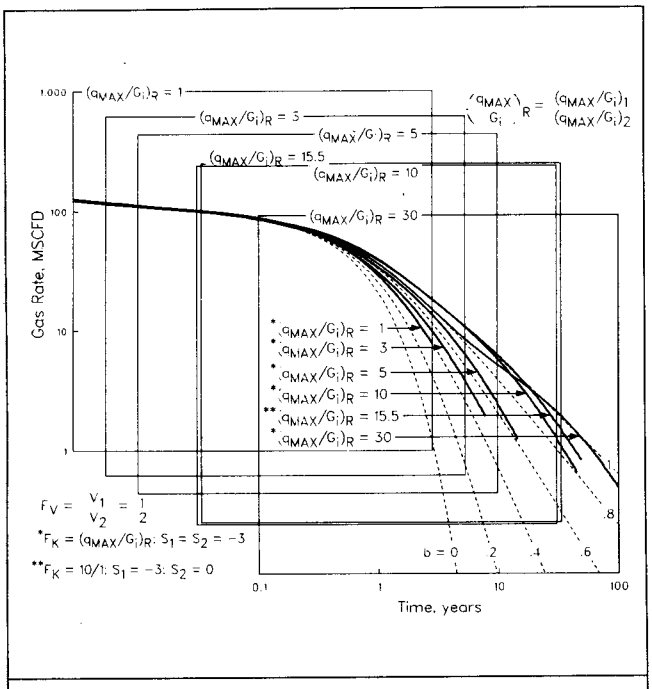

Fig. 16—Composite well declines for $(q_{max}/G_i)_R$ between 1 and 30 and $F_V = 1:2$.

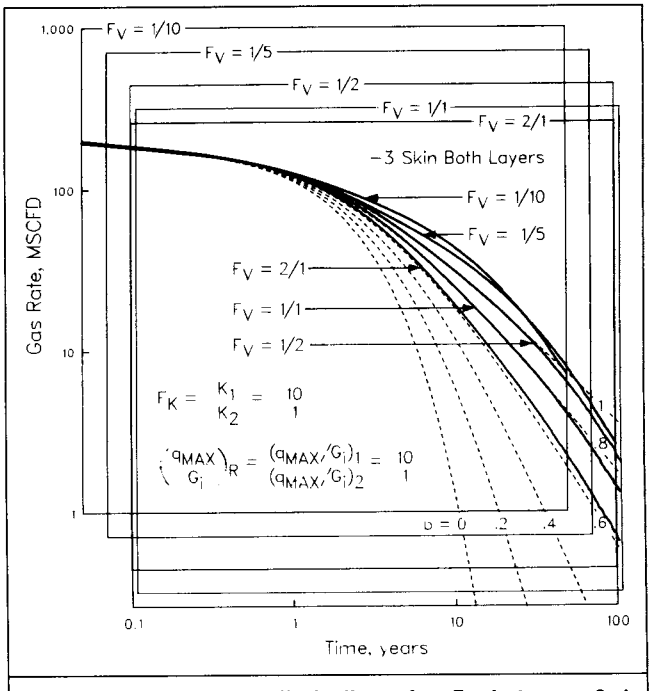

Fig. 17—Composite well declines for F_V between 2:1 through 1:10 and $(q_{max}/G_i)_R = 10$.

When two layers, each characterized by a $b=0.4$, are added together, the composite curve will yield a value of $b>0.4$. Only for the special case in which the ratio of q_{max} to initial gas in place is the same for each layer [$(q_{max}/G_i)_R=1.0$] will the composite curve follow the same depletion stem described by each separate layer. Such cases reduce to a single-layer system.

For a given F_V, the greater the $(q_{max}/G_i)_R$ value, the greater the contrast between early layer producing rates. The low-permeability layer will not contribute a significant fraction of the total rate until the high-permeability layer is depleted. At late time, the total system curve and the low-permeability curve become indistinguishable. For the cases in which $(q_{max}/G_i)_R=F_k=3$ or 10, the composite curve approximates a smooth hyperbolic decline. Differential depletion gives the total rate/time curve the appearance of a single, homogeneous system with a high b value. We know of no other mechanism to explain the occurrence of nearly harmonic decline behavior observed in actual field data.

Note, however, that for cases in which $(q_{max}/G_i)_R > \sim 20$, a double hump appearance is evident in the total rate/time curve. This double-depletion characteristic closely resembles the shape of the type curves developed by Da Prat *et al.*[11] for single-layered naturally fractured reservoirs. The early depletion of the high-permeability layer appears analogous to fracture-volume depletion; the late depletion of the low-permeability layer can be considered analogous to matrix depletion. When attempting to identify a naturally fractured reservoir on the basis of double-depletion rate/time behavior, we must, therefore, consider the possibility of layering with no crossflow. In Monterey reservoirs, for example, the degree of fracturing is highly lithology-dependent and any intralayer fracture/matrix response may be overwhelmed by the layering response among lithologically dissimilar zones of contrasting permeability.

Recall from Fig. 8 that when two separate systems have the same gas in place and share the same F_V and $(q_{max}/G_i)_R$ values, each system will overlie the same $\bar{p}/z$-vs.-G_{pt} curve. **Fig. 14** demonstrates that such systems also will describe similar rate/time curves. In this case, $F_V=1:1$ and $F_k=10:1$ for both systems. For the system shown with open symbols, $s_1=0$ and $s_2=+5$, resulting in $(q_{max}/G_i)_R=15.9$. For the system represented by closed symbols, $s_1=-3$ and $s_2=0$, yielding $(q_{max}/G_i)_R=15.5$. Log-rate-vs.-log-time type curves for these systems exactly match, with a slight shift of both axes resulting from differing layer skins. Note that the total system profiles, shown with square symbols, exactly overlie, each tracing a b stem of 0.8 through 100 years of production.

Fig. 15 shows similar results for two other systems of equal $(q_{max}/G_i)_R$. Both systems assume $F_V=1:2$ and $F_k=10:1$, approximating the values for our field of study. The open symbols refer to the system in which $s_1=+5$ and $s_2=0$, yielding $(q_{max}/G_i)_R=6.3$. The closed symbols identify the system in which $s_1=0$ and $s_2=-3$, resulting in $(q_{max}/G_i)_R=6.4$. Again, composite profiles exactly coincide, this time approximating a b stem of 0.9.

Figs. 14 and 15 reveal that different values of F_V and $(q_{max}/G_i)_R$ produce different b values. **Table 3** shows the complete spectrum of possible Arps b values for various differential-depletion cases. All these results are based on a constant flowing pressure equal to 10% of the initial shut-in pressure. Predictably, for any given F_V, the b value increases as $(q_{max}/G_i)_R$ increases—i.e., as the contrast in layer properties, primarily permeability, becomes more pronounced. For very large values of $(q_{max}/G_i)_R$, however, the double-depletion decline develops and a constant b stem cannot be maintained. At both ends of the $(q_{max}/G_i)_R$ spectrum, therefore, the composite curve collapses to a single-layer profile with $b=0.4$. The highest b values obtained in our study are for $(q_{max}/G_i)_R$ ratios between 10 and 20. Further, for any given $(q_{max}/G_i)_R$, b increases as F_V decreases. Assuming $(q_{max}/G_i)_R=10.0$, for instance, an F_V of 2:1 yields $b=0.65$, an F_V of 1:1 yields $b=0.80$, and an F_V of 1:2 yields $b=1.0$. For very low volume ratios, however, a constant b stem is again impossible to maintain.

Fig. 16 is a type-curve overlay of six $(q_{max}/G_i)_R$ cases, all premising $F_V=1:2$. **Fig. 17** is a similar overlay of five F_V cases, all assuming $(q_{max}/G_i)_R=F_k=10:1$. In both figures, the axes of each individual rate/time plot are shifted so that all cases can be presented on a single Arps depletion type curve. Note that in Fig. 16 the curves generally begin to fall below a fixed b stem at late time. The higher the b stem indicated by the early depletion performance, the earlier in real time this drop-off occurs. For $F_V=1:5$ and 1:10 (Fig. 17), the total system profile briefly exceeds $b=1.0$, only to fall back to a lower b value later in depletion. Eventually, only the low-permeability layer contributes to the total flow rate, and the b value migrates to that of a single layer. Normal wellbore deterioration, liquid loading, etc., experienced even by a single-layer completion, may, in fact, contribute to this migration. With the exception of cases involving low volume ratios, however, our results demonstrate that a fixed b stem will be sufficient for predicting flow rates to a practical economic limit. Nevertheless, caution should be exercised in using a fixed b value to predict

reserves at late time for layered systems. We do not advocate the use of b stems >1.0 for forecasting purposes.

A final point concerns the type-curve-matching procedure used on the curves in Figs. 16 and 17. We were unable to predict analytically exactly where to match each composite rate/time curve with a total system kh. An approximate match could be obtained by first estimating q_{dD} using kh_t and $\overline{\mu B}$, and then shifting the curve from left to right along the time axis. The problem lies in estimating the time to pseudosteady state for a layered system, making the t_{dD} match point difficult to evaluate. Further, the total system PV cannot be estimated exactly from a type-curve match of the total rate profile. If a gas well exhibits $b>0.5$, indicating the presence of a layered system, individual layer volumes may be estimated by graphically desuperposing the total system curve from the high-permeability layer with a trial-and-error procedure.

Discussion

Most reservoirs consist of several layers with reservoir properties varying to some degree between layers. Whether crossflow exists may be of considerable importance in long-term forecasting. If crossflow exists, layers can be combined into a single equivalent layer with the average reservoir properties of the crossflowing layers. Even if crossflow does not exist, layers can still be combined into an equivalent single layer if each has the same diffusivity properties, or q_{max}/G_i. It should also be possible to reduce multilayer systems into equivalent two-layer systems for rate/time analysis or production forecasting. We also found that limited-crossflow cases can behave similarly to no-crossflow cases.

In a no-crossflow layered reservoir, or in a well with commingled reservoir completions, to affect long-term production forecasts significantly, a contrast in layer permeabilities must exist. More specifically, the contrast must be in the correlating parameters $(q_{max}/G_i)_R$ and F_V. Reservoirs most likely to develop these contrasts are naturally fractured reservoirs and very thick reservoirs. The Monterey, Spraberry, Altamount-Bluebell, and Austin Chalk have all exhibited depletion-decline exponents approaching 1, suggesting the presence of layering, with little or no crossflow between some or all layers. The early, rapid rate decline observed in such reservoirs is usually interpreted as fracture-volume depletion instead of the differential depletion of the entire naturally fractured layer or layers. Before this study, the double depletion-rate decline illustrated by Da Prat *et al.*[11] was considered to be one of the identifiable responses of naturally fractured reservoirs. This study shows that a no-crossflow layered reservoir, without natural fracturing, can exhibit the same type of response.

Early recognition of a no-crossflow layered reservoir's precipitous rate and pressure/cumulative-production declines would require early individual-layer tests, coring, and a good geological description. The thick shale break observed in all wells in our field of study should have indicated the need for individual-layer tests, both above and below the potential flow barrier. A vertical-permeability test across the shale may also have been warranted. If high- and low-permeability layers are interbedded, however, it may be difficult to test individual layers; pressure-transient tests may reflect only the kh of the high-permeability layer(s).

Obtaining RFT pressures on later development or replacement wells is another method that can be used for the detection of differential depletion in layered reservoirs. Unfortunately, this is a one-time opportunity for a well. The multilayer testing procedures of Ehlig-Economides and Joseph[12] theoretically offer the opportunity to obtain layer pressures, permeabilities, and skins as frequently as necessary to define the pressure-vs.-cumulative-production curve for each layer.

Conclusions

The following conclusions were derived from results calculated by the backpressure-curve/material-balance and the radial-model methods. We believe that all the conclusions are applicable to the gas reservoir described in this paper. Most would be applicable to any no-crossflow layered reservoir.

1. A two-layered-reservoir description reproduces observed rate/time and pressure/cumulative-production performance that a single-layer description cannot reproduce.
2. For all combinations of properties investigated, the rate/time and pressure/cumulative-production performance is not rate-sensitive at practical production rates.
3. Rate/time and pressure/cumulative-production responses can be correlated with $(q_{max}/G_i)_R$ and F_V. The magnitude of b may provide an indication of the permeability contrast and the volume ratio.
4. Arps depletion-decline exponents between 0.5 and 1 can be obtained with a layered-reservoir description given sufficient contrast in layer properties. A depletion-decline exponent >1.0 could not be maintained for any combination of properties investigated.
5. Except for the special cases in which $(q_{max}/G_i)_R$ approaches unity or infinity, the composite-depletion b value is always greater than that of a single-layer system. Field and well rate/time data that exhibit higher-than-expected b values (between 0.5 and 1.0 for gas reservoirs) suggest a layered reservoir system. Large initial percentage declines, not attributable to infinite-acting transient production, followed later by small percentage declines, are a characteristic of high b values and suggest a layered-reservoir response.
6. During the constant-rate production period, the only performance characteristic that can be used to detect layering is the shape of the pressure/cumulative-production plot. The steeper the initial decline in $\bar{p}/z$, the smaller the F_V, G_{i1}/G_{i2}.
7. Different combinations of layer skins can exhibit similar rate/time and pressure/cumulative-production differential-depletion responses.
8. Shut-in pressures obtained for layered reservoirs will track the pressure of the most permeable layer—more specifically, the layer with the highest value of q_{max}/G_i. Extrapolation of a shut-in $\bar{p}/z$-vs.-G_{pt} curve may possibly underestimate the gas in place, G_{it}, at early times and overestimate it at late times. Similarly, semilog extrapolation of early rate/time data will underestimate recoverable reserves. Continuing to extrapolate late rate/time data along a fixed high b value may overestimate recoverable reserves.
9. The total system stabilized backpressure curve of a layered system is not a straight line.
10. A simplified approach with a stabilized backpressure curve and a material-balance equation for each layer yields the same basic results and conclusions as obtained from a radial model.

Nomenclature

b = reciprocal of decline-curve exponent
B = FVF, res vol/surface vol
c_t = total compressibility, psi^{-1}
F_k = layer permeability ratio
F_V = layer volume ratio
G_i = initial gas in place, Bscf
G_p = cumulative gas production, Bscf
h = thickness, ft
J = productivity index
k = effective permeability, md
n = exponent of backpressure curve
N_p = cumulative oil production, STB
$\bar{p}$ = average reservoir pressure, psia
p_{cs} = wellhead shut-in pressure, psig
p_i = initial reservoir pressure, psia
p_{wf} = wellbore flowing pressure, psia
Δp = pressure drop, psia
q = flow rate, Mscf/D
q_{dD} = decline-curve dimensionless flow rate
$(q_{max}/G_i)_R$ = ratio defined by Eq. 4
$(q_i)_{max}$ = initial surface flow rate from stabilized curve
$(q^*)_{max}$ = defined by Eq. 9
$q(t)$ = surface flow rate at time t
q_t = total constant rate from Layers 1 and 2
r_e = external boundary radius, ft

r_w = wellbore radius, ft
r_{wa} = effective wellbore radius, ft
s = skin factor, dimensionless
S_w = water saturation, fraction
t = time, days
t_{dD} = decline-curve dimensionless time
T = reservoir temperature, °R
V = volume, ft^3
z = gas compressibility factor, dimensionless
γ_g = gas specific gravity
μ = viscosity, cp
ϕ = porosity, fraction of bulk volume

Subscripts

g = gas
i = initial
o = oil
r = relative
t = total of Layers 1 and 2

Acknowledgments

We thank Phillips Petroleum Co. for permission to publish this paper. We also thank L.K. Thomas, U.G. Kiesow, and B.C. Nolen for their contributions to this study. Special thanks to Kay Patton for the excellent typing of this and other papers previously published.

References

1. Tempelaar-Lietz, W.: "Effect of Oil Production Rate on Performance of Wells Producing from More Than One Horizon," *SPEJ* (March 1961) 26-31; *Trans.*, AIME, **222.**
2. Lefkovits, H.C. *et al.*: "A Study of the Behavior of Bounded Reservoirs Composed of Stratified Layers," *SPEJ* (March 1961) 43-58; *Trans.*, AIME, **222.**
3. Fetkovich, M.J.: "Decline Curve Analysis Using Type Curves," *JPT* (June 1980) 1065-77.
4. Keller, W.O., Tracey, G.W., and Roe, R.P.: "Effect of Permeability on Recovery Efficiency by Gas Displacement," paper presented at the 1949 API Meeting, Tulsa, March.
5. Gentry, R.W. and McCray, A.W.: "The Effect of Reservoir and Fluid Properties on Production Decline Curves," *JPT* (Sept. 1978) 1327-41.
6. Carter, R.D.: "Type Curves for Finite Radial and Linear Gas Flow Systems: Constant-Terminal-Pressure Case," *SPEJ* (Oct. 1985) 719-28.
7. Fetkovich, M.J. *et al.*: "Decline Curve Analysis Using Type Curves—Case Histories," *SPEFE* (Dec. 1987) 637-56; *Trans.*, AIME, **283.**
8. Arps, J.J.: "Analysis of Decline Curves," *Trans.*, AIME (1945) **160,** 228-47.
9. Raghavan, R.: "Behavior of Wells Completed in Multiple Producing Zones," *SPEFE* (June 1989) 219-30.
10. Fetkovich, M.J.: "The Isochronal Testing of Oil Wells," paper SPE 4529 presented at the 1973 SPE Annual Meeting, Las Vegas, Sept. 30-Oct. 3.
11. Da Prat, G., Cinco-Ley, H., and Ramey, H.J. Jr.: "Decline Curve Analysis Using Type Curves for Two-Porosity Systems," *SPEJ* (June 1981) 354-62.
12. Ehlig-Economides, C.A. and Joseph, J.: "A New Test for Determination of Individual Layer Properties in a Multilayered Reservoir," *SPEFE* (Sept. 1987) 261-83.

Authors

Fetkovich

Bradley

Works

Thrasher

Michael J. Fetkovich is staff director and senior principal reservoir engineer for the Drilling & Production Div. of Phillips Petroleum Co. in Bartlesville. He holds a BS degree in petroleum and natural gas engineering from the U. of Pittsburgh and a Dr. ing. degree from the Norwegian Inst. of Technology. Fetkovich was a 1977-78 Distinguished Lecturer discussing Well Testing and Analysis, and he received the 1989 Reservoir Engineering Award. **Mark D. Bradley** is a senior reservoir engineer with Conoco Inc.'s Production Engineering & Research Div. in Houston, specializing in reservoir simulation. Previously at Phillips Petroleum Co., Bradley holds a BS degree in petroleum engineering from the U. of Wyoming. **Adonna M. Works** is a reservoir engineer for the Drilling & Production Div. of Phillips Petroleum Co., studying gas well performance in the Texas panhandle and the Oklahoma Guymon-Hugoton fields. Previously a field engineer, she worked in Oklahoma City and Odessa, TX. Works holds a BS degree in petroleum engineering from the U. of Oklahoma. **Thomas S. Thrasher** is a senior staff reservoir engineering specialist for the Drilling & Production Div. at Phillips Petroleum Co. His primary research interests are advanced decline-curve and pressure-transient analysis. He holds a BS degree in petroleum engineering from the U. of Oklahoma. He currently serves on the SPE Pressure Transient Program Committee and is the Bartlesville Section's membership chairman.

SI Metric Conversion Factors

ft	× 3.048*	E−01	=	m
ft^3	× 2.863 640	E−02	=	m^3
°F	(°F−32)/1.8		=	°C
gal	× 3.785 412	E−03	=	m^3
lbm	× 4.535 924	E−01	=	kg
md	× 9.869 233	E−04	=	μm^2
psi	× 6.894 757	E+00	=	kPa

*Conversion factor is exact.

SPEFE

Original SPE manuscript received for review Oct. 2, 1988. Paper accepted for publication April 9, 1990. Revised manuscript received Dec. 20, 1989. Paper (SPE 18266) first presented at the 1988 SPE Annual Technical Conference and Exhibition held in Houston, Oct. 2-5.